



저작자표시-비영리-변경금지 2.0 대한민국

이용자는 아래의 조건을 따르는 경우에 한하여 자유롭게

- 이 저작물을 복제, 배포, 전송, 전시, 공연 및 방송할 수 있습니다.

다음과 같은 조건을 따라야 합니다:



저작자표시. 귀하는 원저작자를 표시하여야 합니다.



비영리. 귀하는 이 저작물을 영리 목적으로 이용할 수 없습니다.



변경금지. 귀하는 이 저작물을 개작, 변형 또는 가공할 수 없습니다.

- 귀하는, 이 저작물의 재이용이나 배포의 경우, 이 저작물에 적용된 이용허락조건을 명확하게 나타내어야 합니다.
- 저작권자로부터 별도의 허가를 받으면 이러한 조건들은 적용되지 않습니다.

저작권법에 따른 이용자의 권리는 위의 내용에 의하여 영향을 받지 않습니다.

이것은 [이용허락규약\(Legal Code\)](#)을 이해하기 쉽게 요약한 것입니다.

[Disclaimer](#)

Master of Science

혼합현실기반 정형외과수술용
항법시스템 기술 연구

Research on Surgical Navigation System
for Orthopedic Surgery based on Mixed Reality

The Graduate School
of the University of Ulsan

Department of
Biomedical Engineering

Seokbin Hwang

Research on Surgical Navigation System
for Orthopedic Surgery based on Mixed Reality

Supervisor : Dr. Sungmin Kim

A Dissertation

Submitted to
the Graduate School of the University of Ulsan
In partial Fulfillment of the Requirements
for the Degree of

Master of Science

by

Seokbin Hwang

Department of Biomedical Engineering

University of Ulsan, Korea

February 2024

Research on Surgical Navigation System
for Orthopedic Surgery based on Mixed Reality

This certifies that the master's thesis
of Seokbin Hwang is approved.

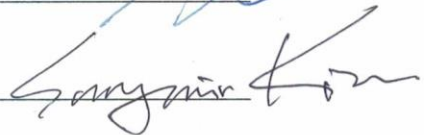
Committee Chair Dr.

Kyo-in Koo



Committee Member Dr.

Sungmin Kim



Committee Member Dr.

Jihwan Woo



Department of Biomedical Engineering

University of Ulsan, Korea

February 2024

Contents

| | |
|--|-----------|
| [Acknowledgement]..... | II |
| [Abstract]..... | III |
| [List of Figures] | V |
| [List of Tables]..... | VI |
| Chapter 1. Introduction | 1 |
| 1.1.Overview..... | 2 |
| 1.1.1. Surgical Navigation for Pedicle screw Placement..... | 3 |
| 1.1.2. Related Works..... | 6 |
| 1.1.3. Objective of Research..... | 7 |
| Chapter II. Surgical Navigation using Mixed Reality | 8 |
| 2.1.System Architecture | 9 |
| 2.1.1. Surgical Planning Module..... | 10 |
| 2.1.2. Surgical Navigation Server and Client..... | 12 |
| 2.2.Evaluation..... | 16 |
| 2.2.1. Experiment Design..... | 19 |
| 2.2.2. Results | 21 |
| Chapter III. Discussion & Conclusion | 25 |
| Reference | 29 |
| 국문요약 | 32 |

[Acknowledgement]

정말 감사합니다. 저에게 가르침을 주신 모든 분들께 감사의 말을 전하고 싶습니다.

김성민 교수님, 덕분에 아득했던 석사학위과정의 종점에 무사히 다다를 수 있었습니다. 코흘리개 학부생 시절부터 석사과정 졸업까지 제 인생의 찰나가 될지도 모르는 시간동안 교수님의 가르침아래 많이 성장했다고 스스로 생각해 봅니다. 연구자로서 뿐만이 아니라 사람으로서, 그리고 인생의 선배로서 교수님께 배운 것들은 앞으로 살아갈 제 삶에 큰 영향을 미칠 것이라고 생각합니다. 감사합니다.

영상유도수술로봇연구실 식구 여러분, 그동안 여러분들과 부대끼며 지낸 시간들은 꽤 오랫동안 추억으로 남을 것 같습니다. 감사합니다.

그리고 항상 저를 믿어 주시고 정신적 기둥이 되어준 사랑하는 부모님, 감사합니다.

2024년 1월 8일

황 석 빈

[Abstract]

Research on Surgical Navigation System for Orthopedic Surgery based on Mixed Reality

Seokbin Hwang

Department of Biomedical Engineering
The Graduate School of University of Ulsan

In orthopedic surgery, spinal fusion is a surgical procedure to treat the patients with intervertebral disc herniation and scoliosis. It rigidly joins two or more vertebrae to support the spine and alleviate pain. For spinal fusion, pedicle screw placement is commonly performed, which inserts screws into bilateral pedicle of vertebra. However, inaccurate screw insertion has been a significant concern of pedicle screw placement because it may give rise to a risk of damaging neurological structures and causing postoperative complications. To minimize the risk of this procedure, surgical navigation systems have been developed, and enhanced the precision of screw placement. However, current surgical navigation systems face several problems including frequent disruptions to the surgeon's attention during operation and complications occur in their depth perception due to the constraints of 2-dimensional (2D) monitors. The objective of this study is to develop a surgical navigation system, aimed at improving these issues using Mixed Reality (MR) technique.

We developed a navigation system that employs a stereo vision-based optical-tracking system (OTS) for tracking surgical instruments, and optical see-through (OST) smart glasses, Microsoft HoloLens, for visualization using MR technique. The proposed system visualizes real time transformation of surgical instrument in terms of spinal model. Using hand and gesture recognition with the MR technique, visualized navigational information can be arbitrarily positioned, rotated, and resized, providing flexibility in visualization. Additionally, proposed system utilizes preoperative surgical planning data to provide visual feedback and guidance to surgeons during procedure.

An orthopedic surgeon performed pedicle screw placement on spinal phantom guided by the navigation system in two different environments using Microsoft HoloLens and 2D monitor. The proposed system was evaluated in terms of procedural time, translational error, angular error, and clinical accuracy. Procedural time with the HoloLens was significantly shorter than with the 2D monitor.

However, there was no statistical difference in translational error, and angular error in two environments. All screws were inserted without cortical violations in both environments.

The navigation system enabled unrestricted visualization, reflecting the perspective of the human eye, and maintained the advantages of MR-based smart glasses. Surgical navigation system feasible for minimally invasive surgery (MIS) should be implemented. Additionally, integrating it with robotic guidance is expected to reduce procedural time.

[Key Words] Mixed Reality, pedicle screw placement, surgical navigation, image-guided surgery

[List of Figures]

| | |
|--|----|
| Figure 1. A 3D rendered CT scan of pre- and postoperative lumbar spine phantom..... | 2 |
| Figure 2. Illustration of an image-guided surgery employing stereo vision-based OTS | 3 |
| Figure 3. Current setup of surgical navigation system displayed on a 2D monitor in operating room .. | 5 |
| Figure 4. General composition of the surgical navigation system..... | 9 |
| Figure 5. A spine phantom and rendered volume CT scan with fiducial points | 10 |
| Figure 6. Visualization of a surgical planning data | 11 |
| Figure 7. Three surgical instruments with their unique arrangement of retroreflective markers and the OTS to track the instruments..... | 12 |
| Figure 8. Collecting a radiopaque fiducial points with the registration tool for the registration | 13 |
| Figure 9. Visual feedback by interaction of the SPP and the VST..... | 14 |
| Figure 10. A 2D canvas-shaped interface for the additional guidance..... | 15 |
| Figure 11. Definition of inserted trajectory..... | 17 |
| Figure 12. 3D rendered CT scans of postoperative CT scan in 3D Slicer..... | 18 |
| Figure 13. Measurement of translational error (TE) and angular error | 18 |
| Figure 14. Two different environments to perform pedicle screw placement using the surgical navigation system | 20 |
| Figure 15. Collision points of the inserted trajectory expressed in 2D SPP at the entry and target points | 22 |

[List of Tables]

| | |
|---|----|
| Table I. Procedural time | 21 |
| Table II. Translational error..... | 23 |
| Table III. Angular error | 24 |

Chapter I. Introduction

1.1. Overview

In orthopedic surgery, patients diagnosed with intervertebral disc herniation and scoliosis can be treated through a surgical procedure known as spinal fusion. Spinal fusion is conducted by orthopedic surgeons or neurosurgeons to join two or more vertebrae at any level in the spine. It gives patients extra support of vertebrae and maintains spinal alignment, for effectively reducing pain and correcting deformities.

Pedicle screw placement is a surgical procedure inserting bilateral screws into pedicle of vertebra commonly performed for spinal fusion (Figure 1). It requires careful planning and high expertise due to its complexity of procedure. Also, precise placement of pedicle screws is important for the stability and safety of the spinal fusion and to avoid damaging spinal nerves and the spinal cord. Because inaccurate screw placement may give rise to neurological complications such as a neurological defects, dura mater violation, and cerebrospinal fluid leakage attributed by medial violation of the spinal canal. Therefore, surgeons use advanced imaging guidance for the surgery, such as fluoroscopy or intraoperative surgical navigation for accurate insertion of screws.

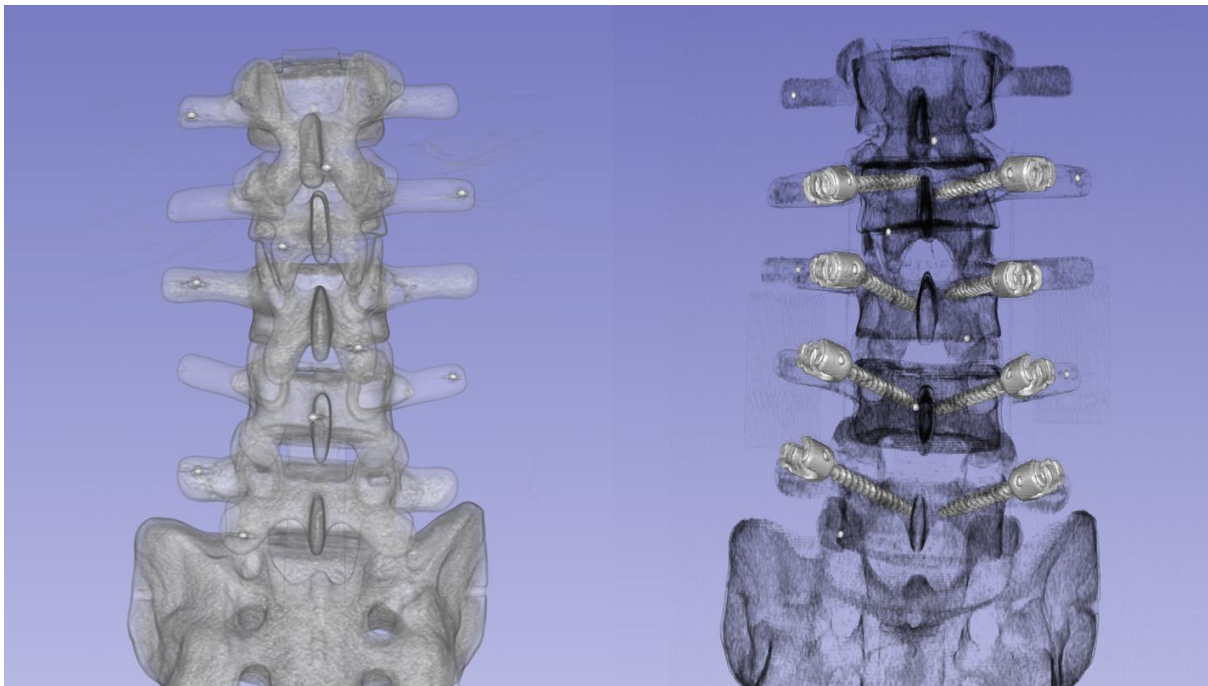


Figure 1. A 3D rendered CT scans of pre- and postoperative lumbar spine phantom. Pedicle screw placement was performed on L2 to L5 bilaterally. (Left - preoperative, Right - postoperative)

1.1.1 Surgical Navigation for Pedicle screw Placement

Advancement of surgical navigation systems has enhanced the precision and safety of surgical procedures. The results of spine surgery in the previous research have clarified clear advantages of surgical navigation systems over conventional freehand techniques, particularly in terms of accuracy, postoperative complications, and revision rate [1-4]. Gelalis et al. [2] reviewed 26 *in vivo* thoracic and lumbar spine pedicle screw placement studies and 17 of them included freehand fluoroscopy guidance, and CT based navigation techniques. They considered the screws is inserted in accurate position if they were fully contained within the pedicle without cortical violation according to the Gertzbein-Robbins classification [10]. Using freehand techniques, reported accuracy varied widely, ranging from 69% to 94%, whereas in CT navigation techniques, accuracy showed a more consistent range from 89% to 100%. In another study, the accuracy of freehand pedicle screw placement significantly varied in *in vivo* cases, with reports ranging from 27.6 to 100%, and in cadaveric cases, the accuracy showed from 12.5% to 95% across all spinal levels according to the Gertzbein-Robbins classification [3, 10]. Furthermore, it has been demonstrated that the variability in accuracy depend on the freehand proficiency of the surgeon, resulting in inconsistent accuracy.

However, surgical navigation systems have evolved to provide intraoperative navigational information that combines medical images, such as computed tomography (CT) or magnetic resonance imaging (MRI), and ultrasound, with real time transformation of surgical instruments, commonly referred to as image-guided surgery (IGS) [11]. Figure 2 shows an optical tracking system (OTS) based IGS. There are fundamental elements of IGS including medical image scan, registration, tracking of surgical instruments [19].

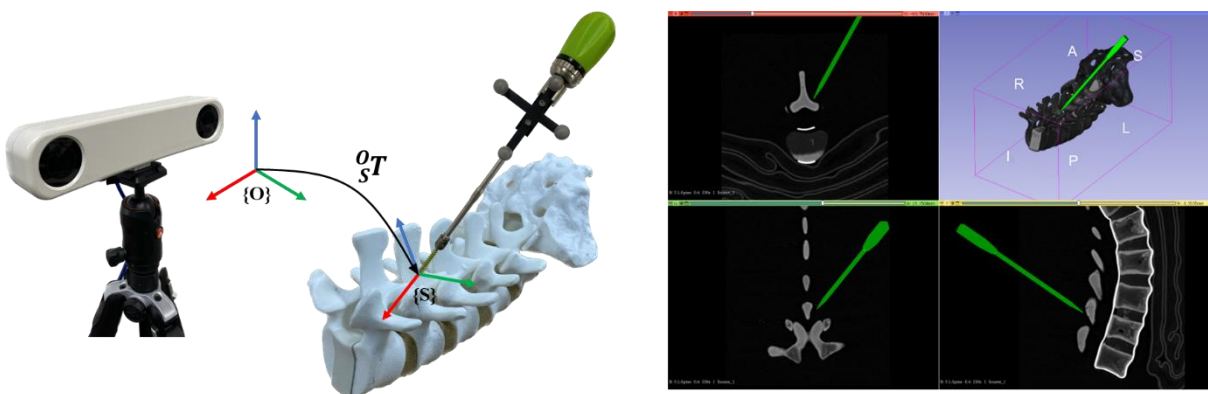


Figure 2. Illustration of an image-guided surgery employing stereo vision-based OTS.

Medical image scan for IGS needs several features different from its normal usage, such as diagnosis, and identification of pathological conditions. They require to define several 3-dimensional (3D) points using anatomical landmarks or fiducials for the registration process.

Registration process is to define a linear relationship between two coordinate systems in physical space (operating room) and digital space (medical images). For this process, two corresponding pointsets should be created in each coordinate system, and preoperative calculation for the linear relationship is conducted. Another approach to perform registration is 3D bone surface matching of pre and intraoperative CT scans [20]. However, accurate registration is significant for ensuring precise guidance of surgical instruments and affects the outcome of surgery as well.

Two different tracking techniques, OTS and electromagnetic tracking system (EMTS) have been widely used to track surgical instruments in IGS. Each of these systems has its own principles, fields of application, and limitations [21]. OTS generally utilizes stereoscopic cameras to derive position and orientation of surgical instrument. This is achieved by identifying a unique optical pattern or an arrangement of markers attached on the instruments and employing reconstruction methods such as, camera calibration, and triangulation [22]. Notable features of OTS include high accuracy of tracking and robustness, as well as a wide tracking range. However, flexible surgical instruments such as catheters cannot be tracked by OTS because the optical markers on the surgical instrument must be rigidly fixed for tracking. Additionally, these markers should remain visible within the line-of-sight of the stereoscopic cameras during surgery, which is a major limitation of OTS. Usually in neurosurgery and spinal surgery, OTS is employed for IGS. EMTS employs electromagnetic field generator to track the position and orientation of electromagnetic sensors, which are typically attached to surgical instruments. Compared to OTS, EMTS is characterized by its non-reliance on line-of-sight constraint. This allows for more flexibility where direct visual tracking is not feasible such as endoscopic surgery and use of catheters. But EMTS has a distinct disadvantage of interferences from metallic and ferromagnetic material within the tracking field.

After the registration process, visualization of navigational information within preoperative medical images generally involves providing resliced planes of volume data along the direction and position of surgical instrument that is being tracked during surgery. Also, a 3D rendered image of volumetric or surface data of patient and target structure is provided with a virtual object represents real time transformation of surgical instrument. Eventually, this allows surgeons to identify the location of target structure in physical space, correct the position and rotation of surgical instrument, and operate on patients with the aid of navigational information during surgery.

However, despite the assistance of IGS, current surgical navigation systems in operating room present ergonomic limitation due to reliance on 2-dimensional (2D) monitor (Figure 3). Surgeons are unable to maintain their line of sight on the surgical field constantly. As a result, attention of surgeon is frequently interrupted during the operation. Also, when using a 3D rendered visualization, the 2D monitor cannot reflect the perspective of the surgeon's eye, complicating depth perception.

To address these issues, mixed reality (MR) and augmented reality (AR) have become valuable in the surgical field for the last years. Compared to conventional visualization through 2D monitor, a head mounted display (HMD) with MR technique has distinct feature of visualizing 3D anatomy structures in exact position of the surgical field reflecting the perspective of human eyes. It can maintain the focus of surgery by keeping depth perception and minimizing attention shifts.



Figure 3. Current setup of surgical navigation system displayed on a 2D monitor in operating room. An orthopedic surgeon performs pedicle screw placement for a pilot study.

1.1.2 Related Works

The well-known limitations of using a 2D monitor setup for IGS have been addressed in previous studies through application of MR and AR techniques [5-8].

Frisk *et al.* [6] conducted a phantom study for percutaneous pedicle screw placement using Curve 1.0 navigation platform (Brainlab AG, Munich, Germany) which employing OTS to track surgical instruments. The software was installed on an HMD, Magic Leap (Magic Leap, Plantation, Florida) to visualize the surgical navigation. Using AR-HMD, it provided a conventional resliced planes along the surgical instrument's position and direction, and spine phantom's anatomical structure with intraoperative surgical planning in the surgeon's field of view.

Some of related studies did not use an OTS to track surgical instruments. Instead, they only utilized the multiple cameras or its own tracking system embedded in HMD which made navigation system more systematically concise.

Butler *et al.* [7] performed percutaneous pedicle screw placement on 165 patients using AR-based surgical navigation, xvision system (Augmedics Inc., Arlington Heights, IL, US). The AR-HMD in this system is equipped with a built-in tracking system to track surgical instruments. And its transparent display overlays intraoperative 3D information directly into the surgeon's field of view.

Libemann *et al.* [5] employed the Microsoft HoloLens to implement a pedicle screw navigation. They utilized the front-facing cameras to track the image marker, and estimate the 3D pose of surgical instruments without use of additional tracking devices such as OTS. Intraoperatively, they sampled a surface point cloud of vertebrae with the surgical instruments to perform registration with preoperative CT scan. Also, they provided a 3D angular deviation between two trajectories of surgical plan and surgical instrument in real-time. They, however, did not visualize the 3D anatomical structure on the surgical field through the MR device. But they reported the visualized navigational information are likely to shift if it is fixed at an exact location when the operator moves.

Müller *et al.* [8] conducted a cadaveric study to perform K-wire insertion on isolated lumbar spines using the same AR based navigation system demonstrated in [5]. The study compared the tracking accuracies of an AR based tracking system and a pose-tracking system (PTS). They demonstrated that AR-based tracking approach was as accurate and precise as PTS. It suggests that AR navigation could lead to a new surgical navigation that requires less infrastructural requirements.

However the tracking approach only relies on AR device forced the surgeon to maintain the fiducial marker within the field of view of the cameras embedded in the HMD. Additionally, the superimposed 3D information may lead to unsatisfactory occlusion of significant anatomical structures [9], and they may not be consistently fixed during operation.

1.1.3 Objective of Research

This study aims to propose a new surgical navigation system for pedicle screw placement using Mixed Reality technique to address the current limitation of AR/MR based systems and design a novel methods for feedback of navigational information. The proposed system visualizes 3D surgical navigation without being restricted to the exact position of surgical field and provides real-time visual feedback on the alignment of surgical instruments with preoperative surgical planning. The proposed system can maintain the aforementioned advantages of depth perception in AR/MR navigation but mitigate the limitations of previous studies.

Chapter II. Surgical Navigation using Mixed Reality

2.1. System Architecture

In this study, a surgical navigation system was designed which consists of a surgical planning module, surgical navigation server and client. Figure 4 shows the comprehensive feature of the surgical navigation system.

The surgical planning module was developed as a built-in module within 3D slicer (www.slicer.org, Version 5.3.0), which is an open-source software utilized for analysis and visualization of medical images. It prepares the necessary information to be visualized during operation, and fiducial pointset for registration. The navigation server, developed with Visual C++ and MFC library, provides the transformation of surgical instruments from a stereo vision-based OTS and performs registration. The navigation client was developed with the Unity 3D (Unity Technologies, San Francisco, California) for the core application and the Mixed Reality Tool Kit (MRTK) (Microsoft, Redmond, WA) for the user interface. It visualizes the surgical navigation including pre- and intraoperative data. Each component is detailed, and the specific hardware and experimental apparatus in the following context.

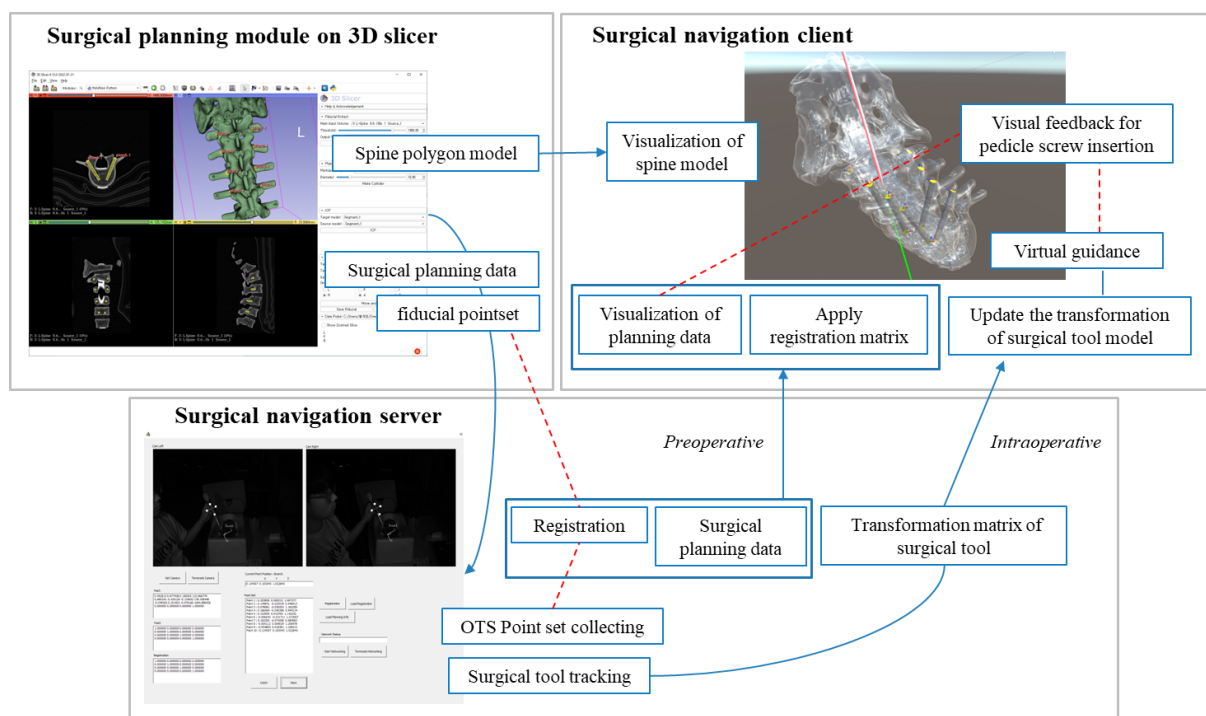


Figure 4. General composition of the surgical navigation system.

2.1.1 Surgical Planning Module

The surgical planning module on 3D Slicer generates a point set of radiopaque fiducials for registration, preoperative surgical planning data sets, and a polygon model of spine.

The preoperative CT scan of a spine phantom with 10 randomly attached radiopaque fiducials (Figure 5a) was performed. In Figure 5b, the Hounsfield unit (HU) of radiopaque fiducials in the preoperative CT ranges to be easily segmented from whole volume data of the spine phantom. The segmentation process was implemented using binary thresholding, 3D gaussian filter, and binary connectivity. The surgical planning module identifies a boundary of each fiducial segment, and central point of each boundary was computed to be a point of the fiducial pointset in the coordinate system of CT (Figure 5b, Figure 5c). Every 10 fiducial points in 3D space in CT volume were collected as matrix p (1).

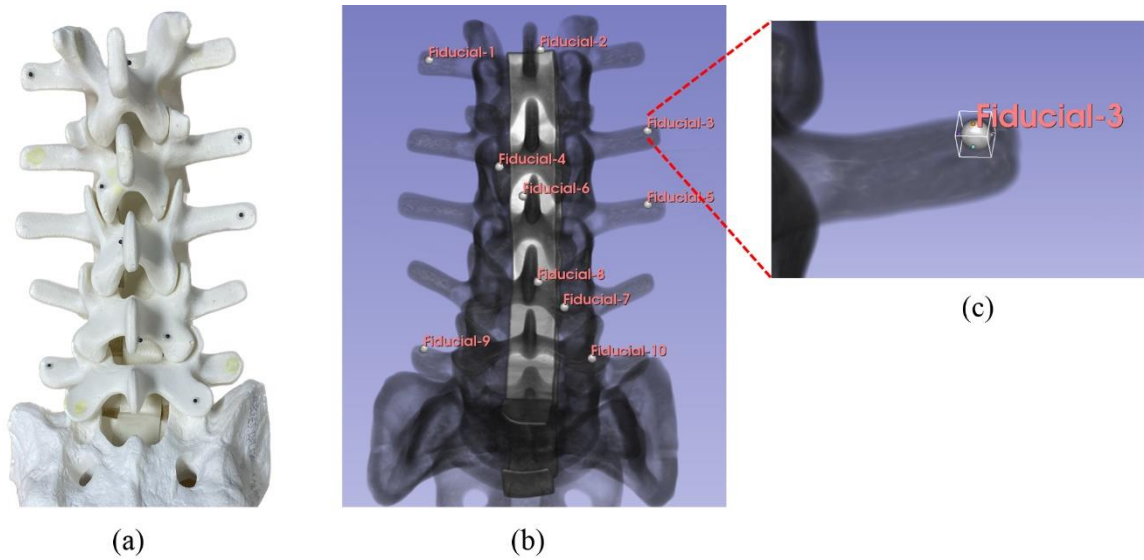


Figure 5. A spine phantom and rendered volume CT scan with fiducial points. a) A spine phantom with 10 radiopaque fiducials. b) A preoperative CT scan of the spine phantom rendered in 3D Slicer. c) The boundary of a segment of a radiopaque fiducial.

$$p = \begin{bmatrix} \text{Fiducial 1} \\ \text{Fiducial 2} \\ \text{Fiducial 3} \\ \vdots \\ \text{Fiducial 10} \end{bmatrix} = \begin{bmatrix} x_1 & y_1 & z_1 \\ x_2 & y_2 & z_2 \\ x_3 & y_3 & z_3 \\ \vdots & \vdots & \vdots \\ x_{10} & y_{10} & z_{10} \end{bmatrix} \quad (1)$$

The preoperative planning data consisted of an entry and a target point in preoperative CT. The entry and target points for each pedicle were defined using the markups tool in 3D Slicer, as illustrated in Figure 6. In this process, surgeons can manually modify the control point of the entry and target points with their clinical background. To correct the entry and target points, a cylinder model with the same radius (3 mm in this study) of pedicle screw was visualized (yellow cylinder object in Figure 6) and overlapped to the preoperative CT. The planning data are basically a 3D vector from an entry to a target point per one pedicle. However, the surgical planning data only defined a directional trajectory and did not consider an exact depth that corresponds to the actual length of the screw, because the depth of screw insertion is determined by the surgeon intraoperatively based on their experiences in surgery.

The spinal model was manually segmented in 3D Slicer. And it is converted into a polygon model directly imported into the MR scene in Unity3D as a polygon model.

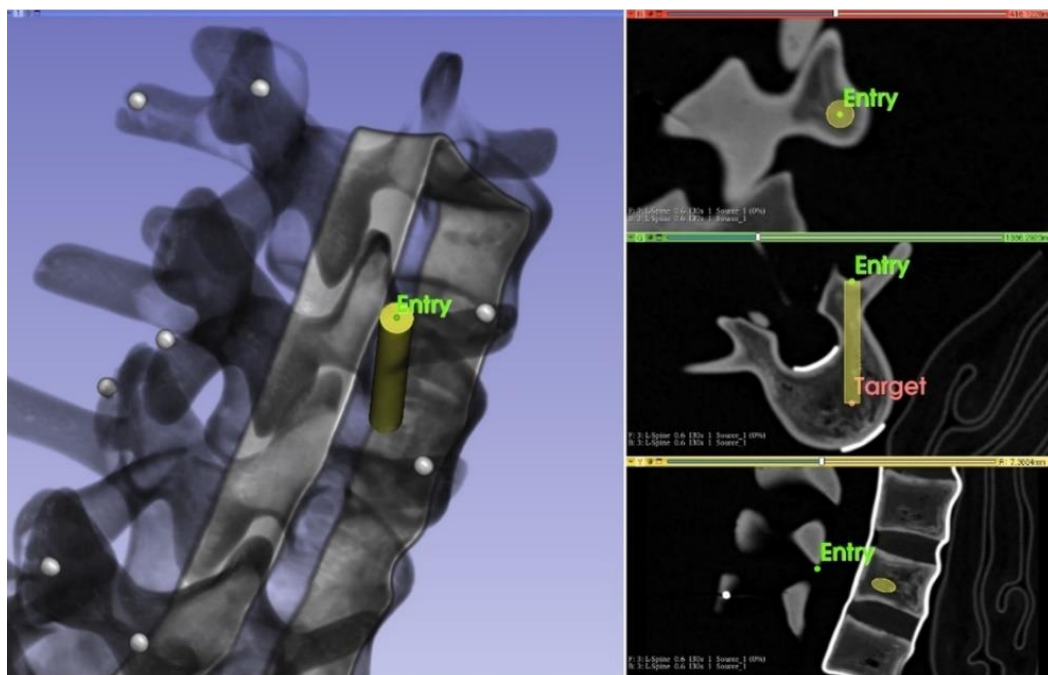


Figure 6. Visualization of a surgical planning data.

2.1.2 Surgical Navigation Server and Client

The surgical navigation server employs a stereo vision-based OTS to track the 3 different surgical instruments (registration tool, the guide drill, and the pedicle screwdriver in Figure 7), i.e., it tracks the position and orientation of surgical instruments and makes them into a 4x4 homogeneous matrix (2) that is denoted as ${}^O_S T$ in Figure 8. The surgical navigation server transmits the preoperative data (surgical planning data, registration matrix) and intraoperative data (transformation matrix of the surgical tool) to the surgical navigation server. All the data is transferred via the TCP/IP network protocol wirelessly.

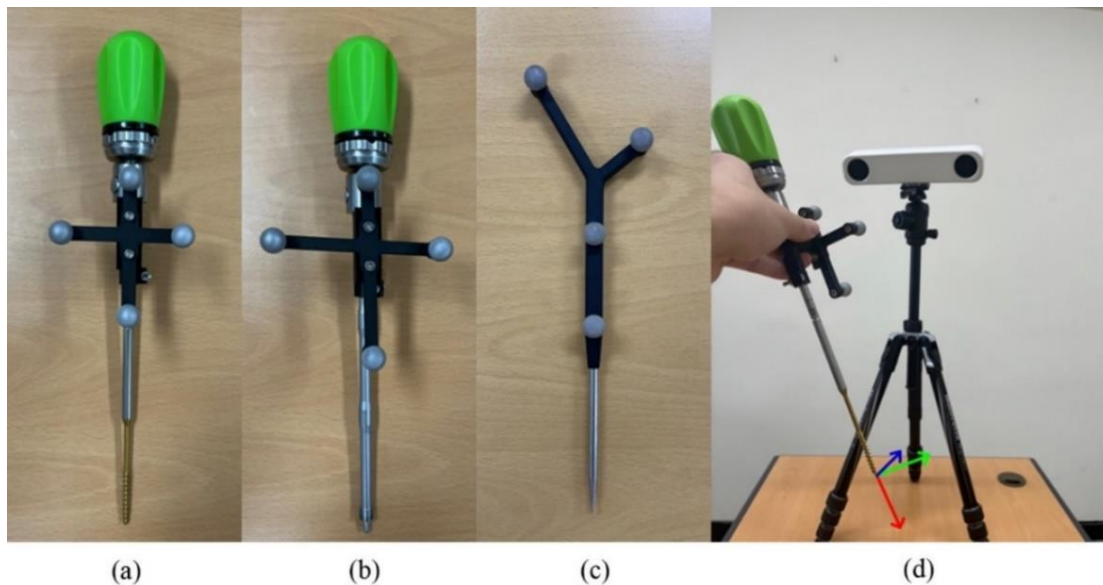


Figure 7. Three surgical instruments with their unique arrangement of retroreflective markers and the OTS to track the instruments. a) Guide drill. b) Pedicle screwdriver. c) Registration tool. d) Example of the tracking pivot point.

Preoperatively, the surgical navigation server collects the 10 fiducial points by directly touching the fiducials (as shown in Figure 8) attached to the spine phantom using the registration tool (Figure 7c). Every last column of ${}^O_S T$ of registration tool is the translational vector of fiducial point in terms of OTS and collected as matrix p' (3) which is used as a moving pointset of registration process. Once, the surgical navigation server takes pointsets from the phantom (p'), and preoperative CT data (p), the registration matrix is computed with a least-squares fitting algorithm [13]. The least-squares fitting is an algorithm that finds the relationship between two corresponding pointsets (4), where R is a 3×3 rotation matrix, T is a 3×1 translational vector, and N is a 3×10 matrix of translational error. The result transformation of the least-squares fitting could be represented in a 4x4 homogeneous matrix $RegMat$ (5), and T_S^I is able to be calculated from matrix multiplication of $RegMat$ and T_S^O in the

surgical navigation client (6). The surgical navigation server sends the *RegMat* and preoperative planning data that were generated from 3D slicer to the surgical navigation client before the operation.

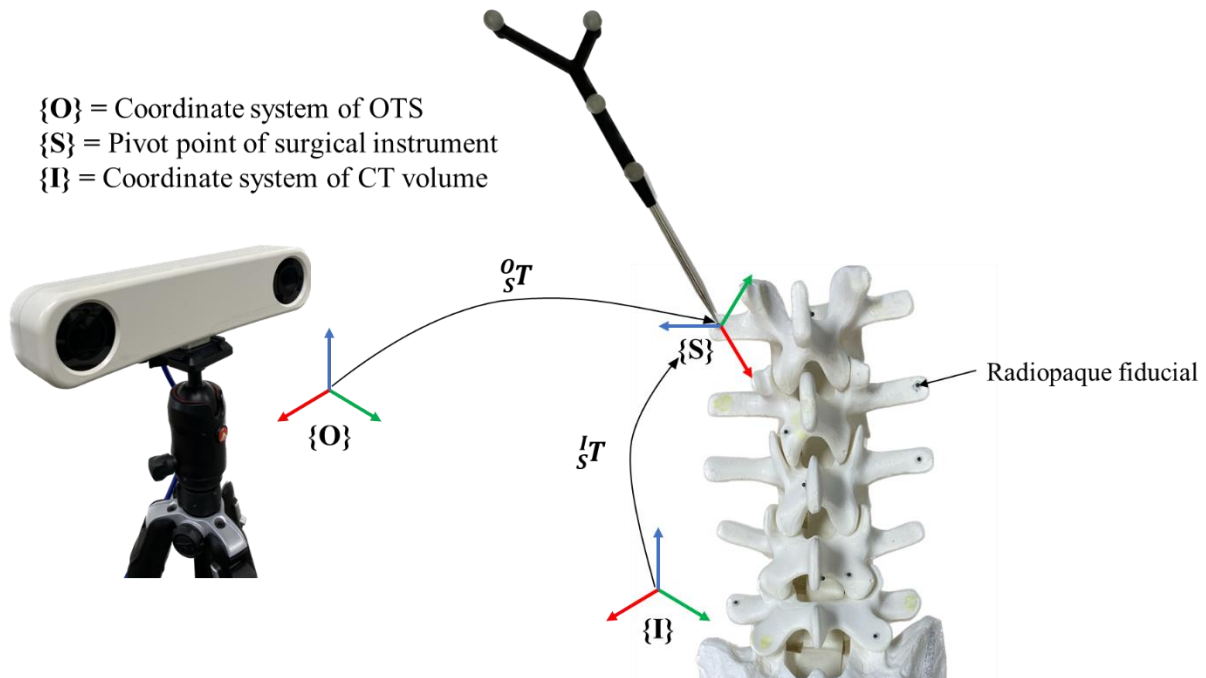


Figure 8. Collecting a radiopaque fiducial points with the registration tool for the registration.

$${}^o_s T = \begin{bmatrix} r_{11} & r_{12} & r_{13} & t_x \\ r_{21} & r_{22} & r_{23} & t_y \\ r_{31} & r_{32} & r_{33} & t_z \\ 0 & 0 & 0 & 1 \end{bmatrix} \quad (2)$$

$$p' = \begin{bmatrix} t_{x1} & t_{y1} & t_{z1} \\ t_{x2} & t_{y2} & t_{z2} \\ t_{x3} & t_{y3} & t_{z3} \\ \vdots \\ t_{x10} & t_{y10} & t_{z10} \end{bmatrix} \quad (3)$$

$$p^T = R(p')^T + T + N \quad (4)$$

$$RegMat = \begin{bmatrix} R & T \\ 0 & 1 \end{bmatrix} = \begin{bmatrix} r_{11} & r_{12} & r_{13} & t_x \\ r_{21} & r_{22} & r_{23} & t_y \\ r_{31} & r_{32} & r_{33} & t_z \\ 0 & 0 & 0 & 1 \end{bmatrix} \quad (5)$$

$$T_s^I = RegMat * T_s^O \quad (6)$$

Intraoperatively, the surgical navigation server constantly sends T_S^O of the guide drill and the pedicle screwdriver to the surgical navigation client in real time.

The surgical navigation client performs comprehensive navigation and visualization by utilizing data received from the surgical navigation server and the spine model from the surgical planning module as well. Additionally, when using the surgical navigation system with the HoloLens, surgeons can adjust the position, rotation, and scale of the displayed navigational information through hand and gesture recognition.

Preoperatively, the surgical navigation client receives preoperative data through the TCP/IP from the surgical navigation server. The surgical planning data consist of a 3D vector per one pedicle, which are the entry point and the target point (Figure 6). The surgical navigation client instantiates two thin (0.1 mm) cylinders that have the same radius as the pedicle screw at the entry and target points as planned in the MR scene and they will be denoted as the surgical planning plane (SPP) in the later context (yellow objects in Figure 9). After completion of the visualization of the SPP, the surgical navigation client receives the registration matrix; $RegMat$ (5) and applies it to the intraoperative transformation of surgical instruments continuously in real time (6), denoted as ${}^I_S T$ in Figure 8. Surgeons can observe the exact location of the virtual surgical tool (VST; object in Figure 9 that changes the color of its surface) in terms of the spine model through the calculation of T_S^I .

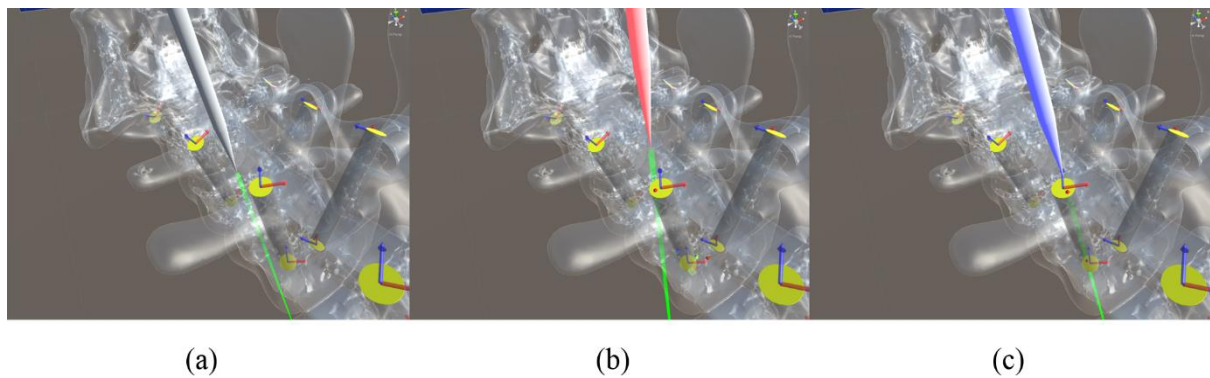


Figure 9. Visual feedback by interaction of the SPP and the VST. a) No visual feedback is given. b) The color of VST's surface turns red when direction of surgical instrument intersects with either entry or target SPP. c) The color of VST's surface turns blue when direction of surgical instrument intersects with both entry and target SPP.

The surgical navigation employs the SPP and VST to provide virtual guidance and visual feedback. It achieves this by projecting a ray from the tip of the VST in its direction. There is a straight line from the VST representing the direction of surgical instrument (the green straight line in Figure 9). According to the case of the direction of surgical instrument that intersects with the SPPs, the color of the VST changes in three conditions (Figure 9). This visual feedback is designed to guide the correction of surgical instruments.

However, it is not the most desired feedback method to correct the position and orientation of the surgical instrument by just changing the color of the VST. Therefore, we employed an additional method for a detailed correction. We assumed the SPP was a 2D plane and displayed the local coordinates of intersection points on an extra space. In Figure 10a, a 2D canvas shaped user interface is displayed in a 3D MR scene. The red sphere dots in Figure 10b are the spots where intersections occurred. The circle and cross shaped cursors indicate the intersection points at the entry and target SPPs, respectively. The blue and red arrows on the SPP in Figure 10a and Figure 10 b are the Z and X axes of the local coordinate system of SPP, respectively, which correspond to the Z and X axes in Figure 15. Through this interface, surgeons can perform detailed correction of the surgical instrument.

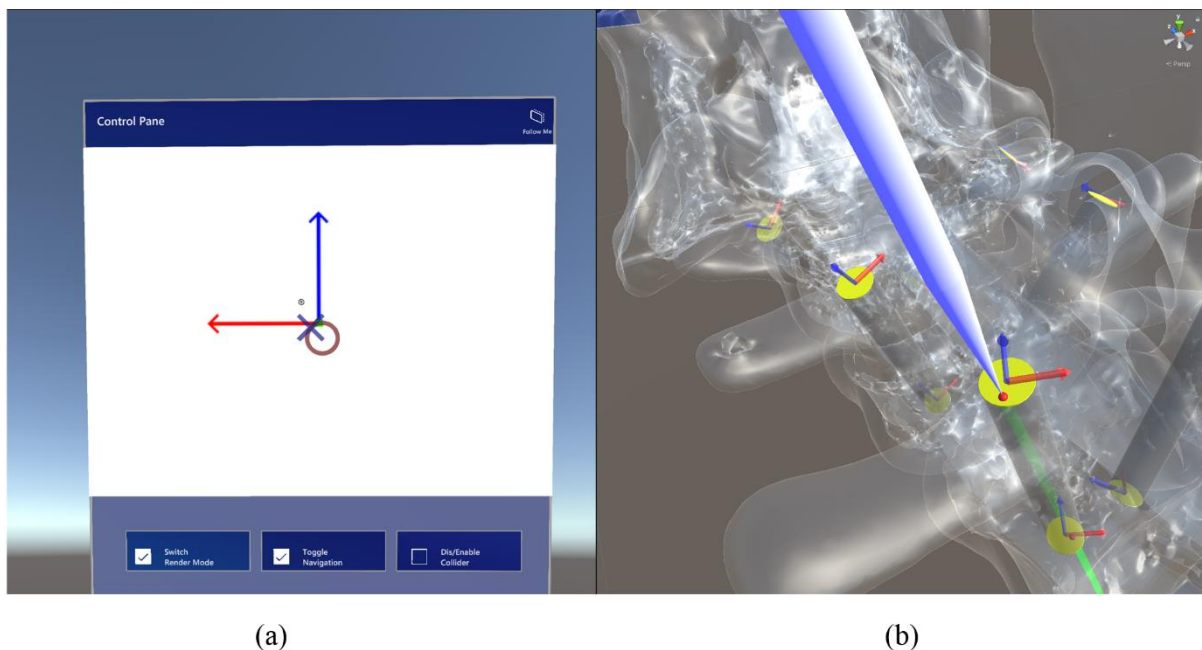


Figure 10. A 2D canvas-shaped interface for the additional guidance. a) An example of 2D expression of the collision points on the canvas shaped user interface. b) An example of collision spots at the entry and target SPPs that correspond to the circle and cross shaped cursor in (a).

2.2. Evaluation

The surgical navigation system of this study was evaluated with translational error, angular error, procedural time, and clinical accuracy. To obtain the translational and angular error inserted trajectories of the pedicle screw were calculated from the postoperative CT.

First, the pre- and postoperative CT scan should be registered. Pre- and postoperative CT both have the same arrangement of radiopaque fiducials. From these fiducials, each fiducial pointset can be determined by the same procedure of fiducial points extraction (Figure 5). Then, the least-squares fitting algorithm [13] was applied to register two corresponding pointsets.

The primary approach for determining the trajectory of the inserted pedicle screw is utilization of the iterative closest point (ICP) algorithm [14].

In the postoperative CT, we segmented the inserted screw with 3D Slicer and converted it a polygon model (Figure 11c). On the other hand, another cylinder with the same dimension of pedicle screw (radius of 3 mm and length of 45 mm) was also instantiated (red cylinder in Figure 11b and 11d). The segmented screw model was designated as the fixed target for the ICP. The cylinder model that was instantiated was aligned with the segmented screw model by the ICP. Eventually, the axial direction of the repositioned cylinder model was regarded as inserted trajectory (Figure 12). With this trajectory, it was possible to measure the translational and angular error.

Translational error refers to the error from the preoperative surgical plan (Figure 13). To measure this, we employed collision detection in Unity3D, a process that is similar to the visual feedback of the navigation method. The inserted trajectory of the pedicle screw is already defined. By projecting a ray along the direction of the inserted screw, two collision points were identified for each pedicle at the entry and target SPPs. Each collision point was subsequently represented in the 2D local coordinate system of each SPP, and the 2D distance from each collision point to the center of the SPP was calculated to determine the translational error.

Angular error for each pedicle screw placement is defined as an angle between planning data and inserted trajectory (Figure 13).

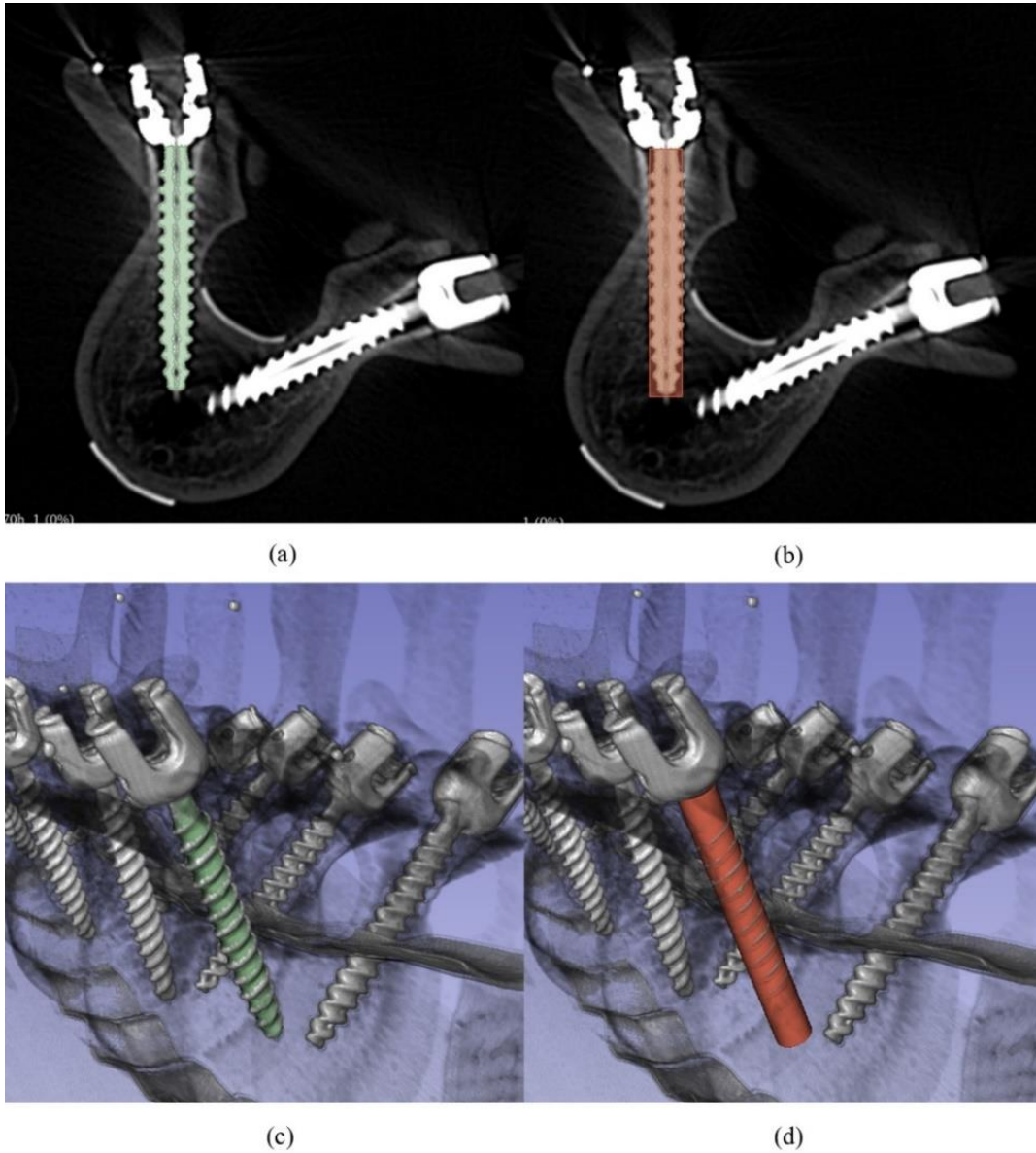


Figure 11. Definition of inserted trajectory. a) A resliced CT plane that shows the segment of the inserted screw. b) A resliced CT that shows an instantiated red cylinder overlapped on (a). c) A rendered volume of the postoperative CT with the segment of the inserted screw. d) A rendered volume of postoperative CT to show the red cylinder that aligns with the segment of the inserted screw.

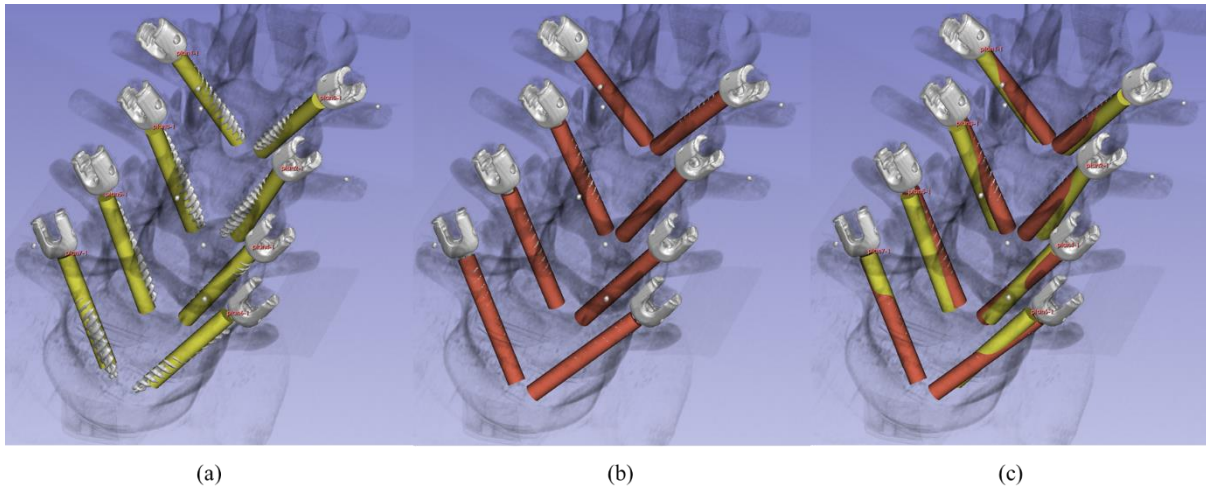


Figure 12. 3D rendered CT scans of postoperative CT scan in 3D Slicer. a) Preoperative surgical plan (yellow cylinder) is visualized with postoperative CT scan. b) Inserted trajectory (red cylinder) is visualized with postoperative CT scan. c) Inserted trajectory and preoperative surgical plan are visualized with postoperative CT scan.

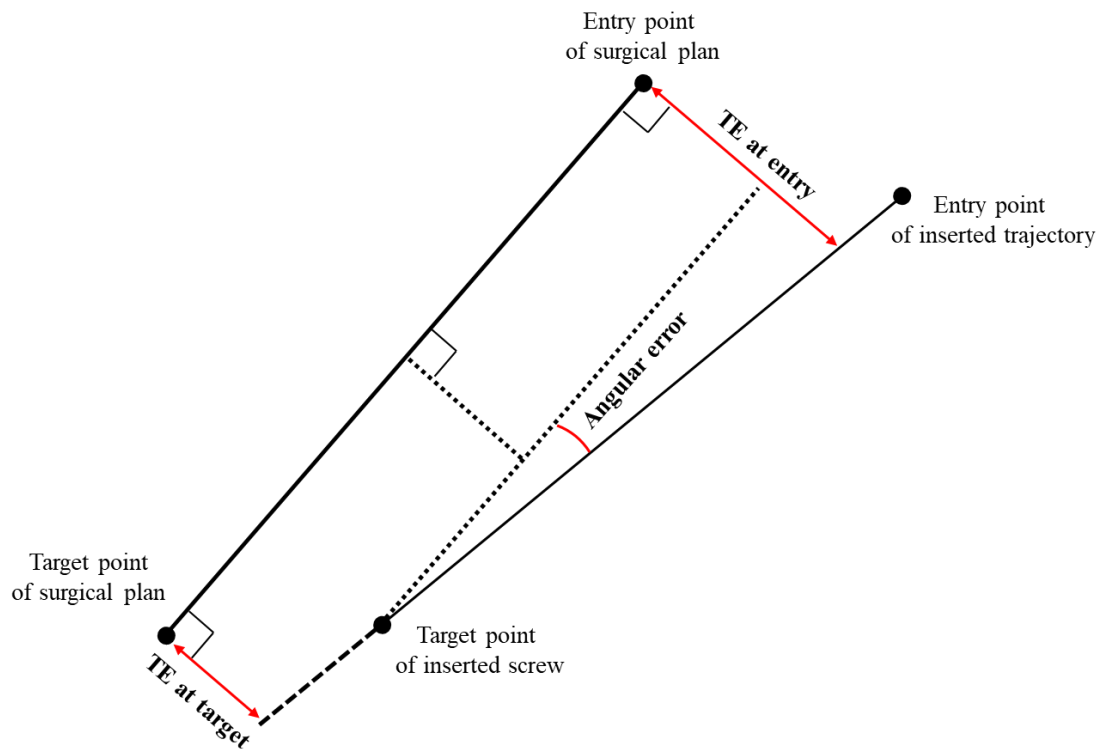


Figure 13. Measurement of translational error (TE) and angular error.

The procedural time for each pedicle screw was the time spent to place a pedicle screw into a pedicle. It is measured from the moment that the surgeon placed the guide drill on the phantom to the pedicle screwdriver detached from the screw.

The Gertzbein-Robbins classification has widely been used to clinically evaluate the postoperative CT. It determines the grade A to E based on a scale of cortical violation for each pedicle as follows: grade A (intrapedicularly inserted), grade B (violation less than 2 mm), grade C (violation less than 4 mm, greater than 2 mm), grade D (violation less than 6 mm, greater than 4 mm), grade E (violation greater than 6 mm).

The translational error is technical accuracy comparing to the preoperative planning data at the entry, and target. Therefore, even if a screw is inserted not perfectly in alignment with the preoperative planning data, it can penetrate through the pedicle without causing cortical violation.

2.2.1. Experiment Design

A desktop PC (AMD Ryzen5 3600XT CPU, 31.9GB RAM) was used to operate the surgical navigation server and the surgical navigation client for the 2D monitor environment. The HoloLens 2 which is an optical see-through (OST) based smart glasses currently commercialized by Microsoft (Microsoft, Redmond, WA) was also used to run the surgical navigation client for the MR environment. We employed an OTS from SKADI (Digitrack, Daegu, Republic of Korea) to track the surgical instruments. Cannulated polyaxial pedicle screws (VIPER, DePuy Synthes) that had a 6.0 mm major diameter and 45 mm length were inserted into lumbar spine phantom (SAWBONES, Vashon, WA).

An orthopedic surgeon performed the pedicle screw placement on four spine phantoms with the surgical navigation in two different environments. In each environment, two spine phantoms were used for the experiment. The surgical navigation can work with both the HoloLens (Figure 14a) and a 2D monitor (Figure 14c). In Figure 14b, the visualized navigation is not overlapped to the spine phantom to avoid undesirable occlusion phenomenon demonstrated in [9].

Before the experiment in each environment, registration was conducted with the registration tool (Figure 7c). The orthopedic surgeon drilled an entry surface in the spine phantom with the guide drill (Figure 7a). Then, the pedicle screw was inserted using screwdriver (Figure 7b). These two steps were performed on eight pedicles from L2 to L5 per spine phantom.



(a)

(b)



(c)

Figure 14. Two different environments to perform pedicle screw placement using the surgical navigation system. a) An environment with the surgical navigation displayed on the HoloLens. b) An example of virtual guidance and visual feedback of the surgical navigation on the HoloLens. c) Another environment with the surgical navigation displayed on a 2D monitor.

2.2.2. Results

A total of 32 pedicles were inserted on four spine phantoms in two different environments.

The procedural time results are summarized in Table 1. For the first two pedicle screws inserted in the environment of the HoloLens at the first experiment, the procedural times were not recorded due to failure in the recording process. Procedural times were 111.3 ± 52.7 s (100.5 [51 - 233] s) and 192.1 ± 104.0 s (164.5 [71 - 478] s) in the environments of the HoloLens and 2D monitor, respectively. The mean procedural time was 42.1% faster in the environment of the HoloLens. The procedural time in each environment were significantly different, with $p < 0.05$ (via t-test).

Table 1. Procedural time

| | HoloLens (s) | 2D Monitor (s) |
|--------------------|--------------|----------------|
| 1st | L2L | N/A |
| | L3L | N/A |
| | L4L | 121 |
| | L5L | 132 |
| | L2R | 208 |
| | L3R | 110 |
| | L4R | 127 |
| | L5R | 111 |
| | L2L | 75 |
| L3L | 59 | |
| L4L | 51 | |
| L5L | 91 | |
| 2nd | L2R | 233 |
| | L3R | 89 |
| | L4R | 81 |
| | L5R | 70 |
| | Average | 111.3 |
| Standard deviation | 52.7 | |

The results for translational error are shown in a scatter plot with a circle, which is shown in a 2D SPP in Figure 15. Each of spine, first and second, are figured with the green and orange scatters respectively. Distances from the center of each scatter point were considered as translational errors and are summarized in Table 2. In the HoloLens, out of sixteen inserted screws, four screws were off the SPP at the entry and ten at the target, respectively (Figure 15). The translational error in the HoloLens was measured 2.14 ± 1.13 mm (2.19 [0.67 - 4.55] mm) at the entry and 3.14 ± 0.90 mm (3.11 [1.47 - 4.60] mm) at the target. In the 2D monitor, three and eight screws were off the SPP at the entry and target out of sixteen pedicle screws. The mean translational error was measured 2.10 ± 0.97 mm (2.18 [0.36 - 4.05] mm) and 3.41 ± 2.16 mm (2.98 [0.79 - 7.94] mm) at the entry and target, respectively. The translational error in the two environments did not show statistically significant differences at either entry or target point, with $p > 0.05$ (via paired t-test).

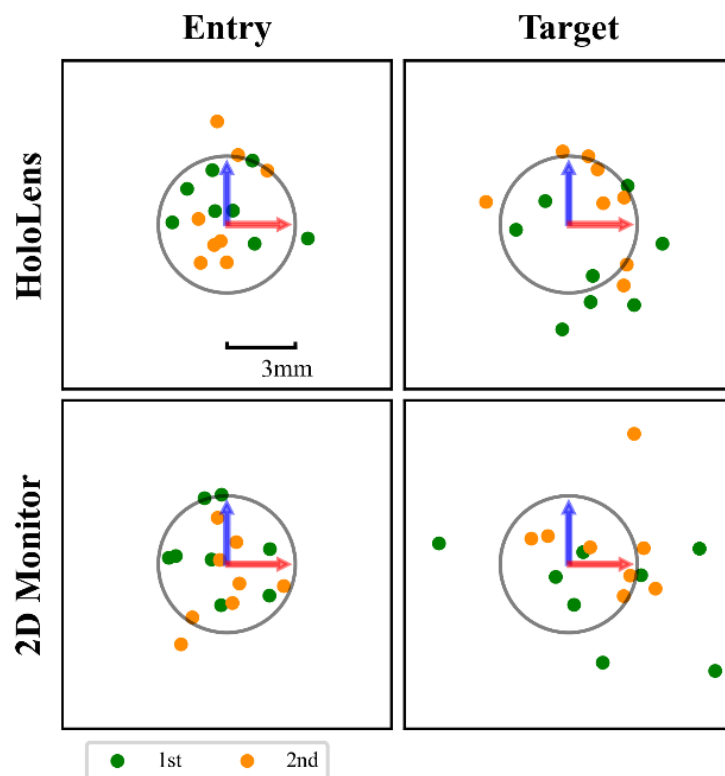


Figure 15. Collision points of the inserted trajectory expressed in 2D SPP at the entry and target points.

Table 2. Translational error.

| | | HoloLens (mm) | | 2D Monitor (mm) | |
|--------------------|-----|---------------|--------|-----------------|--------|
| | | Entry | Target | Entry | Target |
| 1st | L2L | 0.67 | 2.48 | 0.71 | 0.83 |
| | L3L | 3.03 | 4.54 | 3.06 | 7.94 |
| | L4L | 2.47 | 3.09 | 2.56 | 5.76 |
| | L5L | 2.40 | 4.19 | 2.28 | 3.19 |
| | L2R | 2.35 | 3.52 | 3.07 | 4.56 |
| | L3R | 0.80 | 4.60 | 2.00 | 0.79 |
| | L4R | 1.46 | 1.47 | 2.31 | 5.77 |
| | L5R | 3.59 | 2.32 | 1.89 | 1.78 |
| 2nd | L2L | 3.10 | 3.59 | 1.07 | 3.59 |
| | L3L | 1.28 | 3.23 | 0.36 | 3.35 |
| | L4L | 2.04 | 3.12 | 4.05 | 6.4 |
| | L5L | 1.06 | 3.77 | 2.77 | 1.18 |
| | L2R | 4.55 | 2.73 | 2.67 | 2 |
| | L3R | 2.96 | 3.09 | 2.08 | 2.73 |
| | L4R | 0.77 | 2.7 | 1.00 | 2.76 |
| | L5R | 1.66 | 1.78 | 1.72 | 1.55 |
| Average | | 2.14 | 3.14 | 2.10 | 3.41 |
| Standard deviation | | 1.13 | 0.90 | 0.97 | 2.16 |

The angular error is summarized in Table 3. The angular error was measured 6.44 ± 1.94 deg (6.81 [3.81 - 9.24] deg) in the HoloLens environment and it was on average 9.80% more accurate compared to the 2D monitor environment, where it measured 7.14 ± 4.20 deg (6.30 [0.75 - 17.24] deg). There was no statistical difference between two environments, with $p > 0.05$ (via paired t-test).

In both experimental environments, all 32 screws were inserted without any cortical violation.

Table 3. Angular error.

| | HoloLens (deg) | 2D Monitor (deg) | |
|--------------------|----------------|------------------|-------|
| 1st | L2L | 3.81 | 1.67 |
| | L3L | 8.35 | 12.90 |
| | L4L | 4.13 | 10.34 |
| | L5L | 9.24 | 7.74 |
| | L2R | 7.07 | 9.71 |
| | L3R | 6.93 | 3.46 |
| | L4R | 3.87 | 9.967 |
| | L5R | 8.91 | 0.75 |
| | 2nd | L2L | 8.60 |
| L3L | | 4.78 | 5.96 |
| L4L | | 8.31 | 17.24 |
| L5L | | 7.05 | 6.39 |
| L2R | | 3.94 | 6.46 |
| L3R | | 5.97 | 6.07 |
| L4R | | 5.31 | 3.51 |
| L5R | | 6.69 | 6.22 |
| Average | | 6.44 | 7.14 |
| Standard deviation | 1.94 | 4.20 | |

Chapter III. Discussion & Conclusion

This study proposes an MR-based surgical navigation system, which was evaluated by comparing it in two different environments. These environments employed the same navigation system but featured different visualization dimensionalities, as shown in Figure 14.

The visualization method of the navigation system with the MR technique emphasizes efficient and intuitive observation of navigational information reflecting the human eye perspective, rather than solving the attention shift problem which is one of the well-known shortcomings of a conventional 2D monitor environment. Past studies [15, 16] aimed to resolve this issue through AR/MR techniques. Furthermore, according to the reported limitation of fixed virtual object visualized through a MR-HMD, they are likely to shift by even a slight head movement [5]. The visualization method of the designed navigation system in this study avoids the effects from that phenomenon.

Other MR devices based on OST and supports hand and gesture recognition can be also considered for this study. We employed OST based MR device because it can avoid latency issue of Video See-Through (VST) devices. Additionally, OST based MR device like the HoloLens does not require a remote controller to interact with objects in the MR scene. Brining and operating with a remote controller in operating room would be significant problem for clinical application due to the strict sterilization requirements. Hand and gesture recognition in the HoloLens are more suitable for this environment compared to other devices that necessitate the use of remote controllers.

The result of mean procedural time was reasonably favorable to the MR based smart glasses environment, even though attention shifts were allowed in both environments. This demonstrates that the flexibility in visualization and reflecting the human eye perspective make surgical procedures more concise and compensate for the hand-eye coordinate problem as well. Overall, the inserted screw trajectories suggest that the mean translational error at the entry point was relatively more accurate than at the target point for both environments. No statistically significant differences in translational error and angular error were found when comparing the two environments. However, the inserted screw trajectories reached closer to the target SPP and the accuracy at the target point became more diverse and less stable in the 2D monitor environment compared to the HoloLens environment. Therefore, it is understood that the angular error, on average, became greater in the 2D monitor environment.

Previous studies have evaluated navigation systems for pedicle screw placement with technical accuracy and clinical accuracy. Technical accuracy involves translational error and angular error. The Gertzbein-Robbins classification [10] is a primary method to assess clinical accuracy. Burström et al. [17] reported a technical accuracy of instrumentation on pedicles in which the translation error was 1.7 ± 1.00 mm at the entry point and 2.0 ± 1.3 mm at the tip of the surgical instrument. Müller et al. [8] reported a 3D translational error of 3.4 ± 1.66 mm and angular error of 4.3 ± 2.3 deg, using an AR navigation method for K-wire instrumentation on pedicles. In another study, Libemann et al. [5] reported a technical accuracy of bilateral K-wire insertion into lumbar spine, guided by MR-based navigation. Their translational error was 2.77 ± 1.46 mm and the angular error was 3.38 ± 1.73 deg. Their results demonstrate superior technical accuracy compared to this study. However, they inserted only k-wires or drill bits, no actual screws, and calculated the translational error as 3D Euclidean distance. Frisk et al. [6] inserted 24 pedicle screws with AR based surgical navigation and evaluated them technically and clinically. Their translation error measured 1.9 ± 0.7 mm at the entry point and 1.4 ± 0.8 mm at the tip of the surgical instrument. Their angular error was 3.0 ± 1.4 deg.

The surgical navigation system performed registration with the fixed radiopaque fiducials on the spine phantom, which is impractical for an *in vivo* condition. Practically, it is not feasible to perform a preoperative CT scan after making an incision to attach radiopaque fiducials on a human bone structure. Also, it is very important to develop a surgical navigation system as feasible for minimally invasive surgery (MIS). MIS can achieve significant advantages over open surgery, including smaller incisions, less blood loss, shorter hospital stays, and decreased risk of complications [18]. In this study, it is assumed that pedicle screw placement is carried out in an open surgical procedure. Because open pedicle screw placement is considered the standard procedure for long level of spinal fusion procedures. Percutaneous pedicle screw placement can be conducted in limited condition such as short level fusion. During an operation using the proposed navigation system, if the spine phantom is not rigidly fixed on the surgical table, a deformation or space translation of a spine phantom may occur. This can affect the accuracy of registration and result in an inaccurately positioned pedicle screw. In this study, there was no clinical evaluation of the preoperative surgical planning data. The surgeon corrected the preoperative surgical planning data based on their clinical background, but there was no objective assessment of preoperative surgical planning data by another independent surgeon.

The surgical navigation system presents several potential efforts for further improvement of the navigation system. To address the limitations, the surgical navigation system should be designed compatible with percutaneous pedicle screw placement to achieve the advantages of MIS. Additionally, integrating the system with robotic guidance holds promise for reducing procedural times by minimizing hand tremors and time spent on trajectory corrections.

The surgical navigation system which is visualized in an MR environment, can provide flexible manipulation and maintain intuitiveness in observation of navigational information. Visualization of the surgical navigation system in the MR environment achieved shorter procedural times compared to that in the 2D monitor environment, despite allowing attention shifts. The proposed surgical navigation system should improve technical accuracy compared with the current AR/MR-based navigational systems and achieve compatibility with MIS in the future.

References

- [1] B. J. Shin, A. R. James, I. U. Njoku, and R. Härtl, “Pedicle Screw Navigation: A systematic review and meta-analysis of perforation risk for computer-navigated versus Freehand insertion,” *Journal of Neurosurgery: Spine*, vol. 17, no. 2, pp. 113–122, 2012.
- [2] I. D. Gelalis, N. K. Paschos, E. E. Pakos, A. N. Politis, C. M. Arnaoutoglou, A. C. Karageorgos, A. Ploumis, and T. A. Xenakis, “Accuracy of Pedicle screw placement: A systematic review of prospective in vivo studies comparing free hand, fluoroscopy guidance and navigation techniques,” *European Spine Journal*, vol. 21, no. 2, pp. 247–255, 2012.
- [3] V. Kosmopoulos and C. Schizas, “Pedicle screw placement accuracy: a meta-analysis,” *Spine*, vol. 32, no. 3, 2007.
- [4] J. Fichtner, N. Hofmann, A. Rienmüller, N. Buchmann, J. Gempt, J. S. Kirschke, F. Ringel, B. Meyer, and Y.-M. Ryang, “Revision rate of misplaced pedicle screws of the thoracolumbar spine—comparison of three-dimensional fluoroscopy navigation with freehand placement: A systematic analysis and review of the literature,” *World Neurosurgery*, vol. 109, pp. e24-e32, 2018.
- [5] F. Liebmann, S. Roner, M. von Atzigen, D. Scaramuzza, R. Sutter, J. Snedeker, M. Farshad, and P. FÜRnstahl, “Pedicle screw navigation using surface digitization on the Microsoft HoloLens,” *International Journal of Computer Assisted Radiology and Surgery*, vol. 14, no. 7, pp. 1157–1165, 2019.
- [6] H. Frisk, E. Lindqvist, O. Persson, J. Weinzierl, L. K. Bruetzel, P. Cewe, G. Burström, E. Edström, and A. Elmi-Terander, “Feasibility and accuracy of Thoracolumbar Pedicle screw placement using an augmented reality head mounted device,” *Sensors*, vol. 22, no. 2, p. 522, 2022.
- [7] A. J. Butler, M. W. Colman, J. Lynch, and F. M. Phillips, “Augmented reality in minimally invasive spine surgery: Early efficiency and complications of percutaneous pedicle screw instrumentation,” *The Spine Journal*, vol. 23, no. 1, pp. 27–33, 2023.
- [8] F. Müller, S. Roner, F. Liebmann, J. M. Spirig, P. FÜRnstahl, and M. Farshad, “Augmented reality navigation for spinal pedicle screw instrumentation using intraoperative 3D imaging,” *The Spine Journal*, vol. 20, no. 4, pp. 621–628, 2020.

- [9] Y. Liu, M.-G. Lee, and J.-S. Kim, "Spine surgery assisted by augmented reality: Where have we been?," *Yonsei Medical Journal*, vol. 63, no. 4, p. 305, 2022.
- [10] S. D. Gertzbein and S. E. Robbins, "Accuracy of pedicular screw placement in vivo," *Spine*, vol. 15, no. 1, pp. 11–14, 1990.
- [11] W. Eric L. Grimson, R. Kikinis, F. A. Jolesz, and P. McL. Black, "Image-guided surgery," *Scientific American*, vol. 280, no. 6, pp. 62–69, 1999.
- [12] N.-F. Tian and H.-Z. Xu, "Image-guided pedicle screw insertion accuracy: A meta-analysis," *International Orthopaedics*, vol. 33, no. 4, pp. 895–903, 2009.
- [13] K. S. Arun, T. S. Huang, and S. D. Blostein, "Least-squares fitting of two 3-D point sets," *IEEE Transactions on Pattern Analysis and Machine Intelligence*, vol. PAMI-9, no. 5, pp. 698–700, 1987.
- [14] Z. Zhang, "Iterative Closest Point (ICP)," *Computer Vision*, pp. 433–434, 2014.
- [15] J. Traub, T. Sielhorst, S.-M. Heining, and N. Navab, "Advanced display and visualization concepts for image guided surgery," *Journal of Display Technology*, vol. 4, no. 4, pp. 483–490, 2008.
- [16] P. Zhang, H. Liu, H. Li, and J. J. Wang, "The application of navigation system based on augmented reality head-mounted devices in spine surgery," *Neuroscience Informatics*, vol. 2, no. 2, p. 100076, 2022.
- [17] G. Burström, R. Nachabe, O. Persson, E. Edström, and A. Elmi Terander, "Augmented and virtual reality instrument tracking for minimally invasive spine surgery," *Spine*, vol. 44, no. 15, pp. 1097–1104, 2019.
- [18] C. L. Goldstein, K. Macwan, K. Sundararajan, and Y. R. Rampersaud, "Perioperative Outcomes and adverse events of minimally invasive versus open posterior lumbar fusion: Meta-analysis and systematic review," *Journal of Neurosurgery: Spine*, vol. 24, no. 3, pp. 416–427, 2016.
- [19] D. E. Azagury, M. M. Dua, J. C. Barrese, J. M. Henderson, N. C. Buchs, F. Ris, J. M. Cloyd, J. B. Martinie, S. Razzaque, S. Nicolau, L. Soler, J. Marescaux, and B. C. Visser, "Image-guided surgery," *Current problems in surgery*, vol. 52, no. 12, pp. 476–520, 2015.

- [20] C. H. Ewurum, Y. Guo, S. Pagnha, Z. Feng, and X. Luo, "Surgical Navigation in Orthopedics: Workflow and System Review," *Advances in Experimental Medicine and Biology*, vol. 1093, pp. 47-63, 2018.
- [21] M. Mehling, "Implementation of a low cost marker based infrared optical tracking system," M.S. thesis, Vienna University of Technology, 2006.
- [22] A. Sorriento, M. B. Porfido, S. Mazzoleni, G. Calvosa, M. Tenucci, G. Ciuti, and P. Dario, "Optical and Electromagnetic Tracking Systems for Biomedical Applications: A Critical Review on Potentialities and Limitations," *IEEE Reviews in Biomedical Engineering*, vol. 13, pp. 212–232, 2020.

[국문 요약]

혼합현실기반 정형외과수술용 항법시스템 기술 연구

황 석 빈
의용생체공학과
울산대학교 대학원

정형외과 수술에서 척추고정술은 추간판 탈출증과 척추측만증 환자를 치료하는 수술로 두개 이상의 척추를 연결하여 외부적 지지를 제공하고 척추 배열을 교정할 수 있다. 척추경 나사못 삽입술은 양측 척추경에 나사못을 식립하는 수술이며 척추고정술을 위해 사용되는 일반적인 수술이다. 그러나 이 과정에서 부정확한 나사의 삽입은 척추관의 신경 구조의 손상과 수술 후 합병증을 발생시킬 수 있기 때문에 해당 수술의 주요한 요인으로 알려져 왔으며, 이러한 위험을 최소화하고 수술의 정확도 및 정밀도를 높이기 위해 수술용 항법시스템이 개발되어 왔다. 하지만 현재 수술용 항법시스템은 수술실 내부에서 2차원 모니터를 통해 의료진에게 제공되기 때문에 집도의의 주의력 분산을 야기하고 3차원 정보를 관찰하는 집도의의 눈의 원근을 반영하지 못한다는 한계점이 있다. 본 연구는 이러한 문제점을 개선하고자 혼합현실 (Mixed Reality) 기술 기반의 스마트 글래스 장치를 활용한 수술용 항법 시스템을 제안한다.

우리는 수술용 항법시스템을 개발하기 위해 스테레오 비전 (stereo vision) 기반 광학식 추적 장치와 마이크로소프트사의 혼합현실 기반 스마트 글래스 홀로렌즈 (Microsoft HoloLens)를 사용하였다. 이는 각각 실시간 수술도구의 자세 추적과 혼합현실 기술을 활용한 정보의 가시화를 위해 사용되었다. 제안된 시스템은 실시간 수술도구의 자세를 실제 수술대상의 모델과 함께 가시화하며, 혼합현실 기술의 손 및 제스처 인식 기능을 활용하여 가시화된 정보의 위치, 회전, 크기를 사용자 임의로 조작할 수 있다. 또한, 제안된 시스템은 수술 전 계획 정보를 사용하여 수술 중 의료진에게 시각적 피드백과 가이드를 제공한다.

제안된 시스템은 2차원 모니터, 홀로렌즈를 사용하여 가시화한 각각의 환경에서 요추 척추 모형을 활용한 실험을 통해 수행시간, 위치 오류, 각도 오류, 그리고 임상 정확도 측면에서 평가되었다. 홀로렌즈를 사용한 실험의 경우 2차원 모니터를 사용한 환경보다 통계적으로 유의미한 차이를 나타내는 짧은 수행시간을 기록하였으며 두가지 환경에서 모두 척추관을 침범하지 않는 안전한 경로로 나사못이 식립되었다.

제안된 수술용 항법시스템은 사용자의 원근을 반영하여 3차원 정보를 가시화하며, 그 위치, 회전, 크기를 제한하지 않는다. 향후 제안된 시스템이 경피적 (Percutaneous) 척추경 나사못 삽입술에 적용되는 형태로 개발된다면 최소 침습 수술 (Minimally Invasive Surgery)의 장점을 취할 수 있을 것으로 기대된다. 또한, 로봇 가이드와 통합된 수술용 항법 시스템은 수술 수행 시간을 단축시키는 데 기여할 것으로 기대된다.

[주제어] Mixed Reality, pedicle screw placement, surgical navigation, image-guided surgery